Solar Energy Materials & Solar Cells 134 (2015) 194–198

Contents lists available at ScienceDirect

Solar Energy Materials & Solar Cells

journal homepage: www.elsevier.com/locate/solmat

8.7% Power conversion efficiency polymer solar cell realized with non-chlorinated solvents

G. Susanna [a], L. Salamandra [a], C. Ciceroni [a], F. Mura [b,c], T.M. Brown [a], A. Reale [a], M. Rossi [b,c], A. Di Carlo [a], F. Brunetti [a,*]

[a] CHOSE (Centre for Hybrid and Organic Solar Energy), Department of Electronic Engineering, University of Rome Tor Vergata, via del Politecnico 1, 00133 Rome, Italy
[b] Center for Nanotechnology for Engineering (CNIS), University of Rome La Sapienza, P.le A. Moro 5, 00185 Rome, Italy
[c] Department of Basic and Applied Sciences for Engineering, University of Rome La Sapienza, Via Antonio Scarpa 16, 00161 Roma, Italy

ARTICLE INFO

Article history:
Received 8 August 2014
Received in revised form
21 November 2014
Accepted 22 November 2014

Keywords:
Polymer bulk-heterojunction solar cell
Low band-gap
Inverted architecture
Non-chlorinated solvent

ABSTRACT

The use of environmental friendly solvents for the fabrication of solution processed organic photovoltaics is a key issue to scale up the technology. Nowadays however, toxic and harmful chlorinated solvents are largely used in polymer solar cell laboratory research. In this work we successfully reached high solubility and miscibility of the low band gap polymer Poly[[4,8-bis[(2-ethylhexyl)oxy]benzo[1,2-b:4,5-b′]dithiophene-2,6-diyl][3-fluoro-2-[(2-ethylhexyl)carbonyl]thieno[3,4-b]thiophenediyl]] (PBDTTT-E-F, commonly known as PTB7), blended with [6,6]-Phenyl-C71-butyric acid methyl-ester ([70]PCBM fullerene derivative) in a non-chlorinated solvent (Dimethylbenzenes also known as Xylenes). We studied the solar cells realized depositing blend solutions based on various Xylenes (*ortho*, *para* and an isomeric mixture from technical grade) achieving high power conversion efficiencies up to 8.7%.

1. Introduction

Low band-gap polymer-based Bulk-Heterojunction (BHJ) organic solar cells (OSCs) have gained significant attention in the last few years, since the possibility to reach power conversion efficiencies (PCE) higher than 9% for a single layer device [1], and to overcome the target of 10% in a tandem structure [2].

Such high efficiency values together with the native opportunity to scale up the realization process on large area at relatively low costs [3], push the BHJ-based photovoltaics to the top of the future feasible renewable energy technologies.

There are many applicable printing techniques (screen, spray, gravure and ink-jet printing, blade and slot-die coating) [4–6] that can be implemented on roll-to-roll (R2R) [7,8] mass production systems that make this technology attractive and even if the reproduction of the performance of a laboratory device on large area (module) is still an issue [9], some paper demonstrated feasibility to overcome this obstacle [10,11].

However, the use of toxic and harmful chemicals inside formulation of polymer/fullerene blend printed inks, in particular chlorinated solvents (*chloro-* and *dichloro-benzene*) [12], is currently the most common choice for high performance devices [1]. The use of these solvents leads to an increase of the overall costs of the large area process because the huge volume quantities involved in the scaling-up are significant and require appropriate design of the production line with suitable safety equipment and specific disposal of hazardous waste [13]. In this context, the challenge is to obtain high efficiencies with the use of inks based on safe and industrial compatible solvents.

In this work, we successfully obtained high performance BHJ inverted solar cells based on a mixture of PTB7 and [70]PCBM (1:1.5), blended at 2.2 wt% in different formulations of Dimethylbenzene. In particular, we compared devices realized with *ortho*-Xylene (*o*-Xy), *para*-Xylene (*p*-Xy), plus a mixture of Xylene isomers (*mix*-Xy), resulting in a chlorine-free processing – except for the small amount (3% v/v) of 1,8-diiodooctane (DIO) additive [14]. We were able to reach an overall high PCE of 8.73%, 7.87% and 8.22%, respectively for *o*-Xy, *p*-Xy and *mix*-Xy. As reference cell in conventional Chlorobenzene (Cb) solution, we obtained a PCE of 7.9%. Furthermore the transmittance of the best performing cell (in the visible+near IR range), resulted increased of the ~21% more than the reference device; thus, it results an enhanced transparency for the final device. This feature would play an important role both for eventual building integration and for the realization of a tandem architecture where the transparency of the first stacked device is a critical issue to achieve high efficiency [15–17].

* Corresponding author. Tel.: +39 672597366.
E-mail address: francesca.brunetti@uniroma2.it (F. Brunetti).

http://dx.doi.org/10.1016/j.solmat.2014.11.042
0927-0248/

2. Experimental

2.1. Materials

PEIE (Polyethylenimine, 80% Ethoxylated, $M_w \sim 70{,}000$ g, Aldrich) was diluted in 2-methoxyethanol (0.2 wt%), as described in literature [15,18,19]. PTB7 and [70]PCBM (99.99%) were purchased from Solarmer and Solenne BV, respectively. *Ortho*-Xylene, *para*-Xylene, molybdenum (VI) oxide (MoO_3, 99.98% powder) and silver (Ag, wire $\geq$ 99.99%) were purchased from Sigma Aldrich. The Xylenes isomeric blend mixture is technical grade.

2.2. Device fabrication

The devices are realized on ITO glass-covered substrates (Kintec $\sim 8\Omega/\square$), patterned with wet-etching in hydrobromic acid and cleaned in ultrasonic bath with acetone and ethanol (10 min each step). The substrates are covered with PEIE deposited via spin-coating in air under chemical hood at 5000 rpm for 60 s. The PEIE is thermal treated at 120 °C on a hot-plate for 10 min in air [20]. Subsequently, samples are transferred inside a glove box with controlled N_2 atmosphere to be spin-coated with PTB7:[70]PCBM mixture. The polymer content of PTB7 and [70]PCBM is combined in a ratio of 1:1.5 and dissolved at 2.2% in weight in three different Xylenes: *ortho*-Xylene (1,2-dimethylbenzene), *para*-Xylene (1,4-dimethylbenzene) and a mixture of Xylenes (technical grade), composed of 90% of ortho, meta, para –Xylene (prevalently ortho-Xylene), and 10% of a mixture of Ethylbenzene and Toluene where the maximum amount of toluene is 0.5%. Finally the 3%v/v of 1,8-diiodooctane (DIO) is added in the solutions that is then put on stirring overnight at room temperature. As reference, a solution in chlorobenzene is prepared in the same conditions. The active blend is spin-coated at 1000 rpm for 120 s, for a resulting thickness of $\sim$80 nm in case of Xylenes films and $\sim$100 nm for chlorobenzene one, and subsequently treated in slight vacuum (10^{-1} mbar) for 20 min to accelerate the drying process and remove residual DIO from thin films [21].

The MoO_3 hole transporting layer (HTL), and the Ag anode are thermally evaporated at 10^{-7} mbar for a final thickness of $\sim$5 nm and $\sim$100 nm, respectively. At the end 8 devices of 0.1 cm^2 are defined on each substrate.

2.3. Characterization

The thickness of layers was evaluated by a profilometer (Dektak 150). The surface morphology of the thin film in different solvent mixtures was taken with an A.P.E. Research Atomic Force Microscope (AFM). Measurements were performed in *Non-Contact* mode with a Silicon tip with a radius of 8 nm, mounted on a cantilever (resonance frequency = 325 kHz) with a spring constant of 40 N/m. Scanning transmission electron microscopy (STEM) images have been realized using a FE-SEM platform (Zeiss, Auriga) with an integrated STEM system.

Device electrical (*J–V*) performances were characterized outside glove box with a source-meter (Keithley 2420) under an AM1.5 Class A ABET solar simulator (100 mW/cm^2); the EQE measures were performed with an IPCE (Incident Photon-to-current Conversion Efficiency) system (IPCE-LS200, Dyers) calibrated with a UV-enhanced Si detector (Thorlabs, 250-1100 nm).

3. Results and discussion

We performed a comparison between Chloro- and Dimethylbenzene (Xylene) solution based devices. We considered an inverted structure (Fig. 1a), largely demonstrated to be more reliable and performing [20,21] with respect to the conventional one. This architecture reached the best record efficiency on a single layer with a low band gap polymer [1].

We focused on the active layer film's performance and characteristics: starting from the same concentration in weight of the PTB7:[70]PCBM material content, we carried out four set of samples changing the solvent. For each solvent we chose the thickness of the active layer that led to the best performing device.

The film deposition resulted in all cases regular and pinhole-free all over the substrate before and after vacuum treatment. A typical characteristic of the Xylenes' films is the frame on the border that makes them distinguishable from chlorobenzene one (Fig. 1b). Despite equal spin-coating parameters, the films deposited from Xylene solvents, present an average thickness of $\sim$80 nm, instead of $\sim$100 nm typical of the Cb one. Differences are evident by looking at the absorbance spectra, where the typical absorption peaks of PTB7 are recognizable in all the films even if they are of lower intensity for Xy films (Fig. 2). The absorbance spectra of Xylene films are completely overlapped due to the similar solvent parameters and thickness of the samples. In addition, the realized samples (Fig. 1b) appear more transparent ($\sim$62% average transmittance) than the Cb counterpart ($\sim$55% average transmittance) even if the performance is comparable, even improved.

This result is explainable considering the different viscosity of the two types of solution. In fact, even if Xylenes and Chlorobenzene have similar viscosity ($\sim$0.80 cP at 20 °C) and similar boiling point (o-Xy 144°, p-Xy 139°, *mix*-Xy 138 °C and Cb 132 °C), they have different densities (Xy = 0.88 g/ml, Cb = 1.11 g/ml). This leads to a different solid content of the solution and therefore to a lower viscosity for the Xylene-based inks.

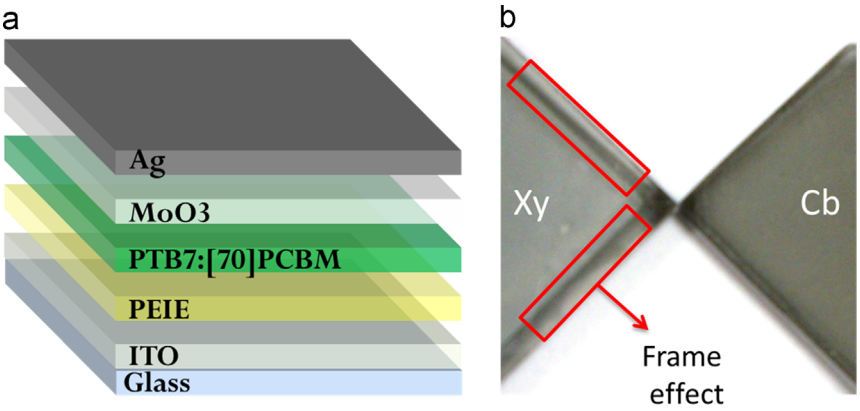

Fig. 1. Stack of the device (a), border effect of Xylene film compared with Chlorobenzene (b).

The *J–V* curves chart shows the best power cell for each set; the best result was a power conversion efficiency (PCE) of 8.74%, with a fill-factor (FF) of 62.2% for the active blend dissolved in *ortho*-Xylene (*o*-Xy). The *para*-Xylene (*p*-Xy) was lower in performance, with a PCE of 7.48% and a FF of 56.4%, whereas the *mix*-Xylene (*mix*-Xy) showed a PCE of 8.22% and a FF of 65.2%, close to *o*-Xy. Except for the *p*-Xy, the devices made with Xylene solutions enhanced the performance with respect to the best chlorobenzene reference cell (Cb), which has a PCE of 7.87% and a FF of 58.5% (Fig. 3).

Given that the pure *o*-Xy isomer is an optimum solvent for the PTB7:[70]PCBM blend, even better than Cb, still it is surprising that also the *J–V* curve in *mix*-Xy is higher, since this is a technical grade formulation, for industrial and generic use, like cleaning and bricolage. The presence of impurities does not seems to influence the solubility, probably for the high concentration of *o*-Xy isomer in this commercial formulation, enough to dissolve properly the solid content present in the blend. This is an important point in the perspective of industrial up-scaling process, since it would allow a substantial decrease in the costs of the materials for inks and an easier feasibility of the process. Table 1 shows the average values of the electrical parameters for each set. The homogeneity of the deposition on the substrate lead to similar cells performance both in case of *o*-Xy and *mix*-Xy; otherwise in case of *p*-Xy the deviation on the device performance is higher, probably due to the different dissolution of the material content.

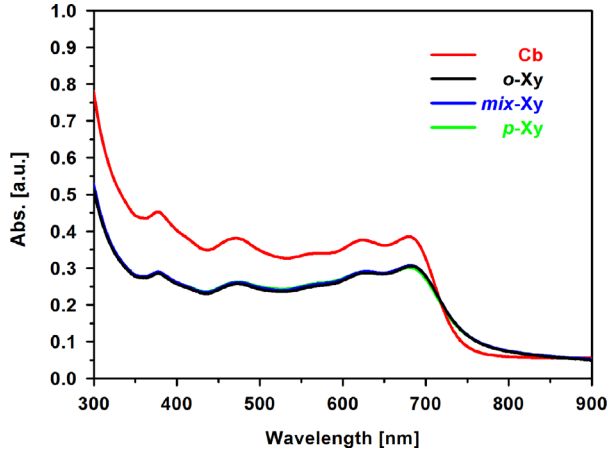

Fig. 2. Absorbance of the PTB7:[70]PCBM in different solvents.

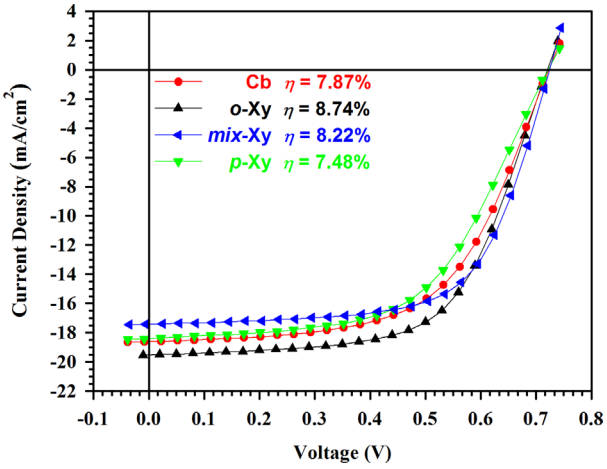

Fig. 3. Comparison of the *J–V* curves for the different solvents.

The uniformity and reproducibility of the *o*-Xy samples exceed the one of Cb; this is also rebounded on the V_{OC}, that is higher and reproducible (see Table 1).

To explain these results a detailed investigation of morphological differences was performed by AFM and STEM analysis. Fig. 4 shows topography images of the polymer/fullerene deposition of the thin film surfaces of Cb and Xy films. In order to perform a better comparison, the images have the same absolute scale. The four surface morphologies are distinguishable: the CB deposition, in Fig. 4a, is characterized from medium size domains with a roughness measured of 2.06 nm RMS and an average height value of 7.74 nm; *mix*-Xy (Fig. 4b) and *o*-Xy (Fig. 4c) topographies present larger size domains. The roughness/median heights for *mix*-Xy and *o*-Xy are 1.92 nm (RMS) / 7.53 nm and 2.55 nm (RMS)/8.74 nm, respectively. The *ortho*-Xylene and the *mix*-Xy show a shape morphology that is similar to the chlorinated sample. On the other hand, the *p*-Xy sample (Fig. 4d), presents very small domains homogeneously distributed, with a roughness of 2.25 nm and heights of 9.05 nm; compared with the other morphologies, the *p*-Xy presents a regular isolation among the domains. The lack of continuity for the charge flow probably influences negatively the fill factor (see Table 1 for details). In Fig. 5a the STEM image obtained for the Cb sample shows a rather uniform distribution of the differences due to the mass contrast that can be interpreted as a homogeneous distribution of the two phases. As a consequence, the donor/acceptor interface can be considered uniformly distributed in the sample. This is due to the presence of the DIO that helps the miscibility of PTB7 and PCBM as it has been already shown in literature [22]. A similar phase distribution is observed for the *mix*-Xy and the *o*-Xy samples (Fig. 5b and c), while for the *p*-Xy sample (Fig. 5d) a slightly less uniform mixture is obtained which could be the reason for the lower performance.

The IPCE measures confirm the good performance of Xylene-based devices, compared to the Chlorobenzene (see Fig. 6). For the Cb solar cell curve, the first shoulder (around 410 nm) and the first peak at ~470 nm are in line with other studies already present in literature [1,22]. Instead, the absence of the peak around 620 nm can be explained considering the absorption properties of the active layer (Fig. 2) which presents a practically flat behavior. This shape has been already observed in literature for a similar percentage of DIO (3% v/v) [23] and could affect the overall charge generation. The IPCE curves of the Xylene-type cells present the same shape in the entire range of wavelength and the increase of measured values as a function of the different xylenes is coherent with the J_{sc} under the sun simulator (see Table 1). Interestingly, it is possible also to observe an increase of the extracted current in the range of 350–450 nm, with a prominent peak at higher energy (~420 nm) where the sun spectra irradiation level is

Table 1
Comparison of the electrical and morphological parameters of the PTB7:[70]PCBM in different solvents.

Solvents	Thickness [nm]	Voc [V]	Jsc [mA/cm^2]	FF [%]	PCE [%]	Max PCE [%]	Roughness (RMS) [nm]	Height [nm]
Cb	~100	0.716 ± 0.006	17.72 ± 0.55	58.5 ± 1.9	7.43 ± 0.27	7.87	2.06	7.74
o-Xy	~80	0.719 ± 0.005	18.58 ± 0.69	61.9 ± 1.9	8.22 ± 0.41	8.74	2.28	8.74
mix-Xy	~80	0.725 ± 0.005	17.34 ± 0.22	63.6 ± 1.5	8.00 ± 0.19	8.22	2.01	7.53
p-Xy	~80	0.715 ± 0.010	17.54 ± 1.53	56.1 ± 2.62	6.73 ± 0.70	7.48	2.25	9.05

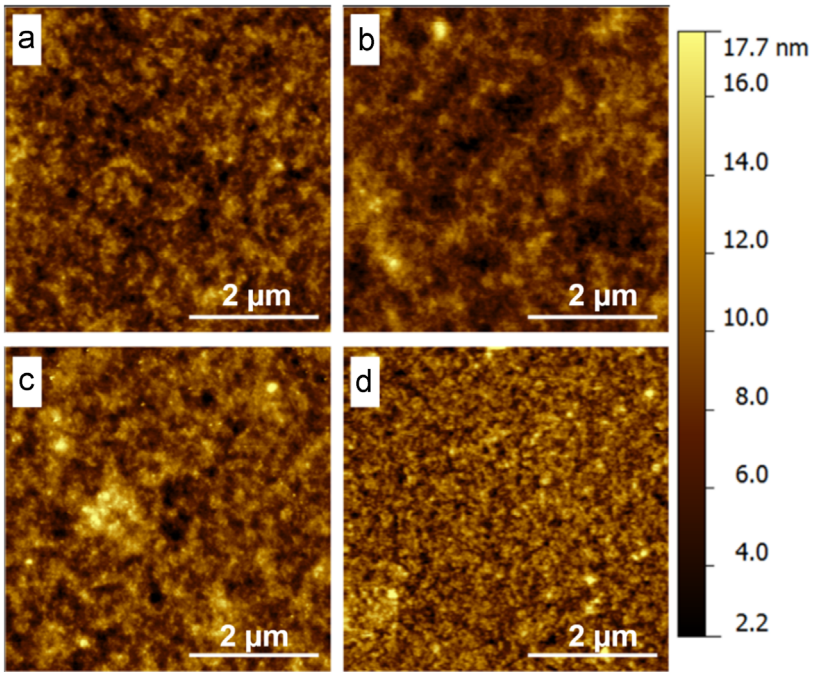

Fig. 4. AFM images of each film: Chlorobenzene (a), mixture of Xylenes (b), *ortho*-Xylene (c), *para*-Xylene (d).

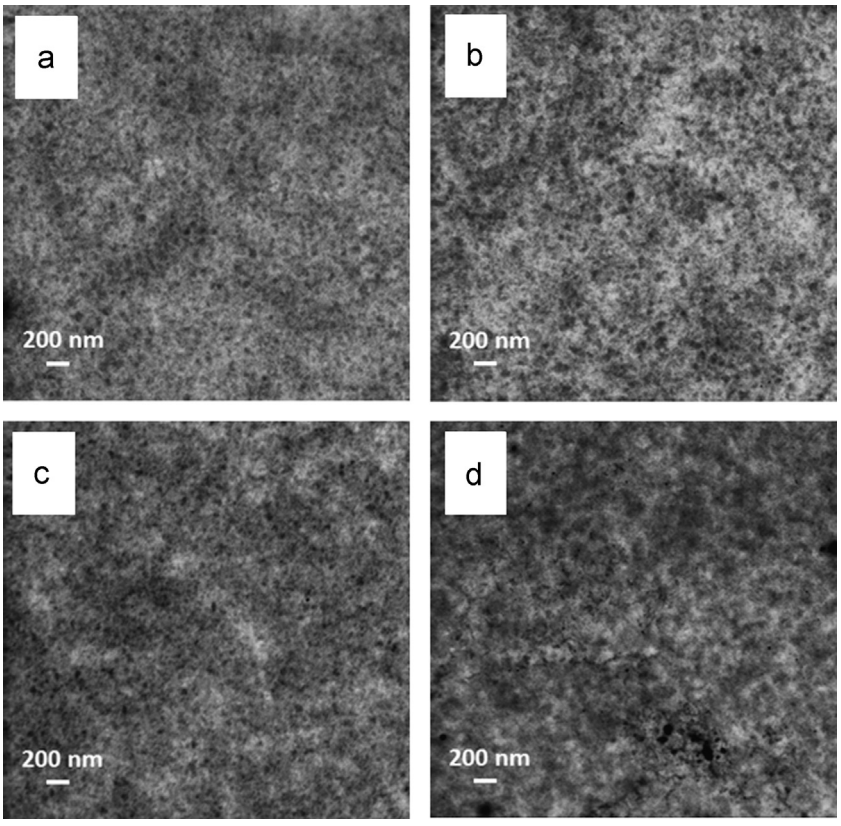

Fig. 5. STEM images of each film: Chlorobenzene (a), mixture of Xylenes (b), *ortho*-Xylene (c), *para*-Xylene (d).

higher. This peak, which has been observed for all the realized Xylene devices, could be due to the way the film is formed using a different solvent respect to Chlorobenzene. Moreover, it is probably the reason of similar levels of current respect to the Cb samples even if the active layers are thinner. To date, there is no evidence about the reason of this change in shape; further studies are required to clarify this issue.

4. Conclusions

In conclusion, we have shown the feasibility of high efficient solar cells using non-chlorinated solvents. We demonstrated high solubility and miscibility of the blend PTB7:[70]PCBM in various Xylene isomers, obtaining devices with high performance, over the

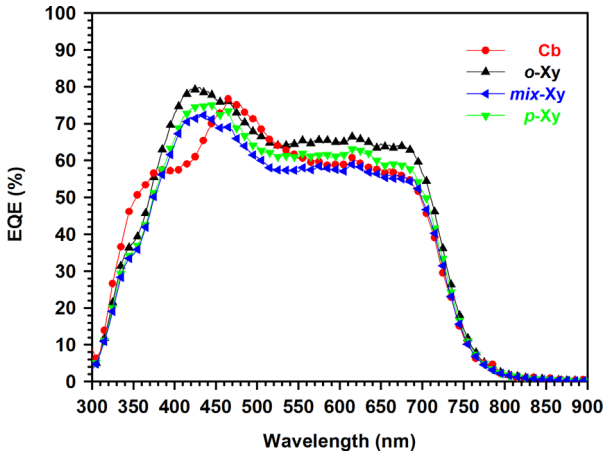

Fig. 6. Comparison of IPCE curves for the different solvents.

8% of PCE also with common industrial isomeric blend with low purity. Best device comes from *o*-Xy, with a high power conversion efficiency of 8.7% that overcomes the reference in chlorobenzene. The transparency is also improved and this feature would play an important role both for eventual building integration and for the realization of tandem architecture where the transparency of the first stacked device is a critical issue to achieve high efficiency.

The switch to an easier to handle, less toxic and harmful solvent represents an important result to scale up organic solar cells paving that way for large area and high efficiency devices.

Acknowledgments

This work was funded by the European Union under Contract no. 309201 “GO-NEXTs”, CHOSE (Centre for Hybrid and Organic Solar Energy) “Polo Solare Organico Regione Lazio” and University of Rome “Tor Vergata” and P.P.G Italy Business Support Srl. We also thank SEQUEL's project for instrumental support.

References

[1] Z. He, C. Zhong, S. Su, M. Xu, H. Wu, Y. Cao, Enhanced power-conversion efficiency in polymer solar cells using an inverted device structure, Nat. Photon. 6 (2012) 591–595.
[2] J. You, L. Dou, K. Yoshimura, T. Kato, K. Ohya, T. Moriarty, et al., A polymer tandem solar cell with 10.6% power conversion efficiency, Nat. Commun. 4 (2013) 1446.
[3] A.J. Moulé, Power from plastic, Curr. Opin. Solid State Mater. Sci. 14 (2010) 123–130.
[4] L. Dou, J. You, Z. Hong, Z. Xu, G. Li, R.A. Street, et al., 25th anniversary article: a decade of organic/polymeric photovoltaic research, Adv. Mater. 25 (2013) 6642–6671.
[5] F.C. Krebs, Polymer solar cell modules prepared using roll-to-roll methods: knife-over-edge coating, slot-die coating and screen printing, Sol. Energy Mater. Sol. Cells 93 (2009) 465–475.
[6] F.C. Krebs, Fabrication and processing of polymer solar cells: a review of printing and coating techniques, Sol. Energy Mater. Sol. Cells 93 (2009) 394–412.
[7] Y. Galagan, I.G. de Vries, A.P. Langen, R. Andriessen, W.J.H. Verhees, S.C. Veenstra, et al., Technology development for roll-to-roll production of organic photovoltaics, Chem. Eng. Process.: Process. Intensification 50 (2011) 454–461.
[8] N. Espinosa, R. García-Valverde, A. Urbina, F.C. Krebs, A life cycle analysis of polymer solar cell modules prepared using roll-to-roll methods under ambient conditions, Sol. Energy Mater. Sol. Cells 95 (2011) 1293–1302.
[9] R. Po, A. Bernardi, A. Calabrese, C. Carbonera, G. Corso, A. Pellegrino, From lab to fab: how must the polymer solar cell materials design change? – an industrial perspective, Energy Environ. Sci. 7 (2014) 925.
[10] J.E. Carlé, M. Helgesen, M.V. Madsen, E. Bundgaard, F.C. Krebs, Upscaling from single cells to modules – fabrication of vacuum- and ITO-free polymer solar cells on flexible substrates with long lifetime, J. Mater. Chem. C 2 (2014) 1290.
[11] H. Jin, C. Tao, M. Velusamy, M. Aljada, Y. Zhang, M. Hambsch, et al., Efficient, large area ITO-and-PEDOT-free organic solar cell sub-modules, Adv. Mater. 24 (2012) 2572–2577.
[12] M.T. Dang, L. Hirsch, G. Wantz, P3HT:PCBM, Best Seller in Polymer Photovoltaic Research, Adv. Mater. 23 (2011) 3597–3602.
[13] D.J. Burke, D.J. Lipomi, Green chemistry for organic solar cells, Energy Environ. Sci. 6 (2013) 2053.
[14] O. Synooka, K.-R. Eberhardt, H. Hoppe, Chlorine-free processed high performance organic solar cells, RSC Adv. 4 (2014) 16681.
[15] Y. Zhou, C. Fuentes-Hernandez, J.W. Shim, T.M. Khan, B. Kippelen, High performance polymeric charge recombination layer for organic tandem solar cells, Energy Environ. Sci. 5 (2012) 9827–9832.
[16] J. You, C.-C. Chen, Z. Hong, K. Yoshimura, K. Ohya, R. Xu, et al., 10.2% power conversion efficiency polymer tandem solar cells consisting of two identical sub-cells, Adv. Mater. 25 (2013) 3973–3978.
[17] L. Dou, J. You, J. Yang, C. Chen, Y. He, S. Murase, et al., Tandem polymer solar cells featuring a spectrally matched low-bandgap polymer, Nat. Photon. 6 (2012) 180–185.
[18] Y. Zhou, J.W. Shim, C. Fuentes-Hernandez, A. Sharma, K.A. Knauer, A.J. Giordano, et al., Direct correlation between work function of indium-tin-oxide electrodes and solar cell performance influenced by ultraviolet irradiation and air exposure, Phys. Chem. Chem. Phys.: PCCP 14 (2012) 12014–12021.
[19] Y. Zhou, C. Fuentes-Hernandez, J. Shim, J. Meyer, A.J. Giordano, H. Li, et al., A universal method to produce low-work function electrodes for organic electronics, Science (New York, N.Y.) 336 (2012) 327–332.
[20] S. Woo, W. Hyun Kim, H. Kim, Y. Yi, H.-K. Lyu, Y. Kim, 8.9% single-stack inverted polymer solar cells with electron-rich polymer nanolayer-modified inorganic electron-collecting buffer layers, Adv. Energy Mater. 4 (2014) 1301692–1301699.
[21] S.K. Hau, H.-L. Yip, N.S. Baek, J. Zou, K. O'Malley, A.K.-Y. Jen, Air-stable inverted flexible polymer solar cells using zinc oxide nanoparticles as an electron selective layer, Appl. Phys. Lett. 92 (2008) 253301.
[22] Y. Liang, Z. Xu, J. Xia, S. Tsai, Y. Wu, G. Li, C. Ray, L. Yu, For the bright future-bulk heterojunction polymer solar cells with power conversion efficiency of 7.4%, Adv. Mater. (Deerfield Beach, Fla.) 22 (2010) E135–E138.
[23] M. Ito, K. Palanisamy, A. Kumar, V.S. Murugesan, P. Shin, N. Tsuda, J. Yamada, S. Ochiai, Characterization of the organic thin film solar cells with active layers of PTB7/PC 71 BM prepared by using solvent mixtures with different additives, Int. J. Photoenergy (2014)) .